

External magnetic field effect on bifacial silicon solar cell's electric power and conversion efficiency

Issa ZERBO*, Martial ZOUNGRANA, Idrissa SOURABIE, Adama OUEDRAOGO,
Bernard ZOUMA, Dieudonné Joseph BATHIEBO

Laboratory of Thermal and Renewable Energies, Department of Physics, Unit of Training and Research in Pure and Applied Sciences, University of Ouagadougou, Ouagadougou, Burkina Faso

Received: 16.05.2015

Accepted/Published Online: 24.08.2015

Printed: 30.11.2015

Abstract: This article presents a modelling study of external magnetic field effect on a bifacial silicon solar cell's electric power and conversion efficiency.

After the resolution of the magnetotransport equation and continuity equation of excess minority carriers, we calculate the photocurrent density and the photovoltage and then we deduce the solar cell's electric power before discussing the influence of the magnetic field on those electrical parameters.

Using the electric power curves versus junction dynamic velocity we determine the maximum electric power, the operating point of the solar cell, and the conversion efficiency according to magnetic field intensity. The numerical data show that the solar cell's maximum electric power and conversion efficiency decrease with magnetic field intensity.

Key words: Bifacial silicon solar cell, conversion efficiency, electric power, magnetic field, operating point

1. Introduction

The efficiency of a solar cell depends on the electric power delivered to an external circuit but some external factors such as magnetic field, external electric field, and electromagnetic field [1,2] can influence this electric power and so the solar cell quality.

Many studies on electronic and electrical parameters of solar cells under constant magnetic field have been proposed with a one- or three-dimensional approach. Many authors proposed experimental methods to study the magnetic field's effect on solar cell properties. Betser et al. [3] proposed an experimental method to determine InP/GaInAs heterojunction bipolar transistor's photocurrent and minority carriers' mobility under constant magnetic field, while Vardanyan et al. [4] proposed another method for measurement of all recombination parameters (diffusion length, diffusion coefficient, carriers mobility, back surface recombination velocity) in the base region of bifacial solar cells. Erel [5] studied the effect of electric and magnetic fields on the operation of a CdS/CuInSe₂ photovoltaic cell. The experience showed that the open circuit voltage and the electron effective mass increase while the magnetic field intensity increases. Other authors proposed studying the modelling of the magnetic field's effect on solar cell properties. Madougou et al. [6] showed that photocurrent density decreases with the magnetic field for each illumination mode of the bifacial solar cell, while the photovoltage increases with the magnetic field for front side and simultaneous front and back side illumination. I-V characteristics of the bifacial silicon solar cell also decrease with the magnetic field. Zoungrana et al. [7,8], with a three-dimensional

*Correspondence: izerbo@univ-ouaga.bf

approach, studied light concentration bifacial silicon solar cells and they showed a decrease in photocurrent and an increase in photovoltage with the magnetic field. They also noted that magnetic field values greater than 7×10^{-5} T influence carriers' diffusion length and diffusion coefficient.

In this work, we study modelling of the influence of magnetic field intensity on a bifacial silicon solar cell's maximum electric power and conversion efficiency. From the electric power curves versus junction dynamic velocity, we determined the values of maximum electric power delivered by the solar cell to an external circuit and the values of corresponding junction dynamic velocity that we called junction dynamic velocity at the maximum power point, and then we calculated the solar cell conversion efficiency.

2. Theory

2.1. Excess minority carriers' density

We study the base region of a polycrystalline back surface field bifacial silicon solar cell in the quasi-neutral base assumption (Figure 1).

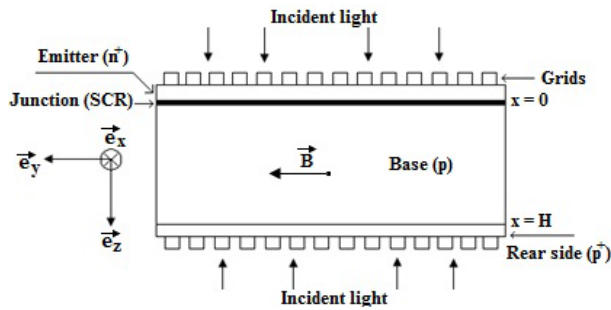


Figure 1. Bifacial silicon solar cell illuminated by multispectral light and under magnetic field influence.

The quasi-neutral base assumption [9] means that the solar cell internal electric field (crystalline electric field) is neglected so that only the junction electric field will be taken into account.

When the bifacial solar cell is illuminated simultaneously on both sides, the solution of excess minority carriers' continuity equation [6], which takes into account carriers' generation, their diffusion under magnetic field, and their recombination, is

$$\delta(x, B) = A \cdot ch\left(\frac{x}{L_n^*}\right) + B \cdot sh\left(\frac{x}{L_n^*}\right) + \sum_{i=1}^3 K_i \cdot \left[e^{-b_i \cdot x} + e^{-b_i(H-x)}\right] \tag{1}$$

with $K_i = -a_i \cdot \left[D_n^* \cdot \left(b_i^2 - \frac{1}{L_n^{*2}}\right)\right]^{-1}$

In these expressions L_n^* and D_n^* are respectively electrons' diffusion length and diffusion coefficient in the presence of a magnetic field. Coefficients a_i and b_i are tabulated values obtained from modelling of the generation rate considered for over all the solar radiation spectrum under Air Mass 1, 5 standard conditions [10] and H is the base thickness.

The excess minority carriers' (electrons) density is completely determined solving the two boundary conditions:

- At the solar cell's junction ($x = 0$)

$$D_n^* \cdot \left. \frac{\partial \delta(x)}{\partial x} \right)_{x=0} = Sf \cdot \delta(x = 0) \quad (2a)$$

- At the solar cell's rear side ($x = H$)

$$D_n^* \cdot \left. \frac{\partial \delta(x)}{\partial x} \right)_{x=H} = -Sb \cdot \delta(x = H) \quad (2b)$$

Sf is the junction dynamic velocity [11] and it quantifies the number of excess carriers that are collected to the junction in a given operating condition (open circuit, intermediate operating point, short circuit).

The junction dynamic velocity (Sf) is the sum of two contributions: the intrinsic junction recombination velocity (Sf_0) related to the losses of carriers at the junction interface and the junction dynamic velocity (Sf_j) that defines the operating point of the cell because it is the carriers' flow imposed by an external load resistance [12].

$$Sf = Sf_0 + Sf_j \quad (3)$$

The solar cell studied in this article is an ideal solar cell and so the losses of carriers at the junction interface are neglected and the intrinsic junction recombination velocity (Sf_0) is null. The junction dynamic velocity (Sf) is equal to the one imposed by an external load resistance (Sf_j) and all the carriers collected at the solar cell's junction cross this junction.

Therefore, when the junction dynamic velocity Sf tends to zero, there is no current flux that crosses the junction and so carriers are stocked on both sides of the junction [13]; that also means that the current flux imposed by an external load resistance is null and this resistance tends to higher value. The solar cell operates in an open circuit. Conversely, when the junction dynamic velocity Sf goes to large values, the maximum of carriers crosses the junction because the external load resistance value tends to zero. The solar cell operates in a short circuit.

Sb , which quantifies the losses of carriers at the solar cell's rear side, is the back surface recombination velocity.

2.2. Photocurrent density

The photocurrent density expression is obtained applying Fick's law at the solar cell junction.

$$J_{ph}(Sf, B) = q \cdot D_n^* \cdot \left. \frac{\partial \delta(x, Sf, B)}{\partial x} \right)_{x=0} \quad (4)$$

The photocurrent density versus junction dynamic velocity curves are plotted in Figure 2 for different values of magnetic field intensity.

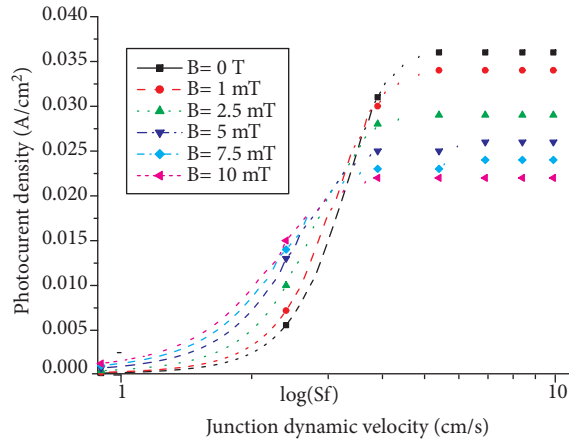


Figure 2. Photocurrent density versus junction dynamic velocity for different values of magnetic field intensity ($L = 0.02$ cm; $H = 0.03$ cm; $D = 26$ cm²/s; $\mu_n = 1000$ cm²/V s).

The curves in Figure 2 show that for large values of junction dynamic velocity (Sf), the photocurrent density is constant and this operating point is the short circuit and the corresponding photocurrent density is short circuit photocurrent density, but for low values of junction dynamic velocity (Sf) the photocurrent is null and this operating point corresponds to the open circuit. One also notes that the short circuit photocurrent density is a decreasing function of magnetic field intensity.

In fact, the strength of Lorentz deviates, towards the lateral surfaces, a part of the electrons photogenerated in the base of the solar cell [8]. Thus, the magnetic field increases carriers' presence near the junction and the quantity of carriers that cross the junction decreases with magnetic field increase [7].

From the analysis of the curves, one notes that the photocurrent density decreases strongly with magnetic field intensity and the values of junction dynamic velocity (Sf) corresponding to short circuit and open circuit conditions decrease with magnetic field increase. Therefore, the magnetic field precipitates the establishment of photocurrent and also the short circuit because while the magnetic field intensity increases, the strength of Lorentz increases and deviates strongly carriers towards the lateral surfaces of the solar cell. This deviation of carriers that increases with magnetic field generates a current in the base of the solar cell.

Applying the concept of junction dynamic velocity initiating the short circuit [14], we determine the values of junction dynamic velocity initiating the short circuit (Sf_{cc}) according to magnetic field intensity.

The results are given in Table 1 below.

Table 1. Junction dynamic velocity initiating the short circuit for different values of magnetic field intensity.

B (mT)	0	1	2.5	5	7.5	10
Sf_{cc} (cm/s)	1.22×10^6	9.243×10^5	2.983×10^5	1.818×10^5	9.543×10^4	6.10×10^4

These results confirm that the values of junction dynamic velocity initiating the short circuit decrease when the magnetic field intensity increases. The magnetic field precipitates the establishment of the short circuit.

2.3. Junction photovoltage

Knowing the excess minority carriers' density, the photovoltage across the solar cell junction is expressed using Boltzmann's relation:

$$V_{ph}(Sf, B) = V_T \cdot \ln \left(N_B \frac{\delta(x=0, Sf, B)}{n_i^2} + 1 \right) \quad (5)$$

V_T is the thermal voltage, n_i is the electrons' intrinsic concentration at thermodynamic equilibrium, and N_B is the base doping density.

We plot in Figure 3 photovoltage versus junction dynamic velocity curves for different values of magnetic field intensity.

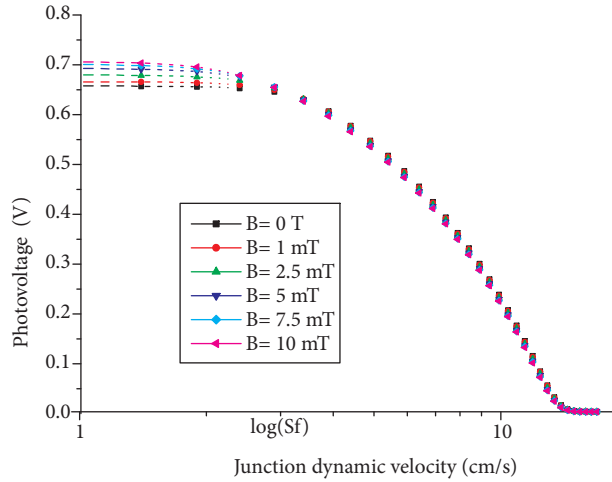


Figure 3. Photovoltage versus junction dynamic velocity for different values of magnetic field intensity ($L = 0.02$ cm; $H = 0.03$ cm; $D = 26$ cm²/s; $\mu_n = 1000$ cm²/V s).

The shapes of the different curves in Figure 3 show that the photovoltage is null for large values of junction dynamic velocity ($Sf \geq 10^{13}$ cm s⁻¹), while it is maximal (open circuit photovoltage) and depends on magnetic field intensity for low values of junction dynamic velocity ($Sf \leq 10^2$ cm s⁻¹). The open circuit photovoltage increases slightly while the magnetic field intensity increases. This behavior of open circuit voltage is the consequence of charge carriers' accumulation across the solar cell junction with magnetic field increase. This accumulation is a consequence of charge due to the Hall effect, which modifies electrons trajectories [4,7] and deviates them towards the lateral surfaces of the solar cell. Thus, the magnetic field increases carriers' presence in the neighborhood of the junction (the open circuit voltage increases slightly) and the quantity of carriers that cross the junction decreases (the photocurrent density decreases strongly) with magnetic field increase [7].

It appears through the magnetic field effect on the solar cell in short circuit and open circuit conditions that the solar cell has resistive behavior under the magnetic field. Thus, the solar cell behaves like a resistance that increases with the magnetic field, resulting in a reduction in the photocurrent and an increase in the open circuit voltage. The resistive behavior of solar cell's base under the magnetic field effect is the magnetoresistance.

3. Simulation results and discussion Solar cell electric power and conversion efficiency

The expression of electric power delivered by the solar cell base to an external circuit is [1,2]

$$P(Sf, B) = V_{ph}(Sf, B) \cdot J_{ph}(Sf, B)_T \quad (6)$$

In this expression, $J_{ph}(Sf, B)_T = q \cdot Sf_j \cdot \delta(x = 0, Sf, B)$ is the photocurrent density that crosses the load resistance.

The variations in electric power versus junction dynamic velocity for different values of magnetic field intensity are plotted in Figure 4.

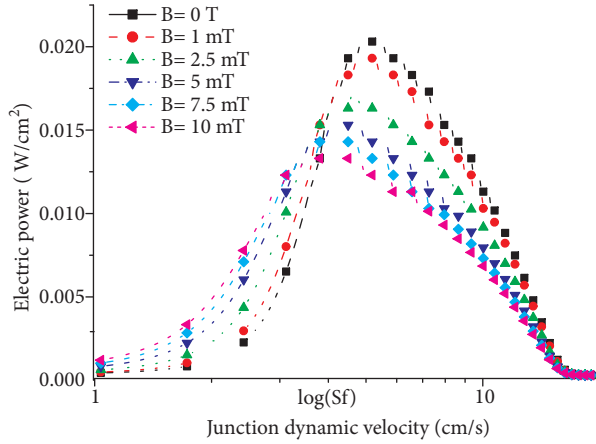


Figure 4. Electric power delivered by the solar cell versus junction dynamic velocity for different values of magnetic field intensity ($L = 0.02$ cm; $H = 0.03$ cm; $D = 26$ cm²/s; $\mu_n = 1000$ cm²/V s).

The shapes of the different curves show that the electric power delivered by the solar cell base is null to the neighborhood of the open circuit and short circuit. Each curve passes by a maximum situated in an intermediate operating point between the open circuit and the short circuit. The maximum electric power decreases with magnetic field increase and it is obtained for values of junction dynamic velocity that moves towards the open circuit (low values of Sf) when magnetic field intensity increases.

Using the electric power curves versus junction dynamic velocity, we determine, according to magnetic field intensity, the values of maximum electric power and the values of corresponding junction dynamic velocity (junction dynamic velocity at the maximum power point) and then we calculate the solar cell conversion efficiency using Eq. (7) below:

$$\eta(B) = \frac{P_{el}(Sf, B)_{\max}}{P_{inc}} \tag{7}$$

P_{inc} is the power of the incident light's flux and $P_{inc} = 100$ mW/cm² in Air Mass 1, 5 standard conditions.

The results are given in Table 2.

Table 2. Maximum electric power delivered by the solar cell, junction dynamic velocity at the maximum power point, and solar cell conversion efficiency for different values of magnetic field intensity.

B (mT)	0	1	2.5	5	7.5	10
P_{max} (mW/cm ²)	19.759	18.757	16.526	14.775	13.810	13.104
Sf_{MPP} (cm/s)	2.928×10^4	1.942×10^4	1.027×10^4	5.727×10^3	3.862×10^3	2.922×10^3
Efficiency η (%)	19.759	18.757	16.526	14.775	13.810	13.104

These results show that the solar cell's maximum electric power and the corresponding junction dynamic velocity (junction dynamic velocity at the maximum power point) decrease while magnetic field intensity increases and that corresponds to a displacement of the solar cell's operating point. The junction dynamic

velocity and the load resistance evolve in reverse senses. Indeed, when the junction recombination velocity decreases one evolves towards the open circuit and the load resistance increases. On the other hand, when the junction dynamic velocity increases, one evolves towards the short circuit and the load resistance decreases.

Thus, the decrease in junction dynamic velocity at the maximum power point with magnetic field increase corresponds to an increase in the charge resistance at the maximum power point.

4. Conclusion

One-dimensional modelling of the magnetic field effect on a bifacial silicon solar cell's maximum electric power and conversion efficiency is presented. It appears that the magnetic field has a large influence on the mobility and concentration of charge carriers that cross the junction. This situation leads to effective magnetic field influence on the solar cell's short circuit photocurrent and open circuit photovoltage; the magnetic field precipitates the establishment of photocurrent and also the short circuit.

We note also that, under magnetic field effect, the solar cell behaves like a resistance that increases with the magnetic field, resulting in a reduction in the photocurrent and an increase in the open circuit photovoltage. This resistive behavior under the magnetic field has been called magnetoresistance.

The numerical data, obtained from the analysis of electric power curves, are evidence of a decrease in the maximum electric power, the junction dynamic velocity at the maximum power point, and the solar cell conversion efficiency. The decrease in junction dynamic velocity at the maximum power point with magnetic field corresponds to an increase in the charge resistance at the maximum power point and so a displacement of the solar cell's operating point.

References

- [1] Zerbo, I.; Zoungrana, M.; Seré, A. D.; Zougmore, F. *IOP Conf. Ser.: Mater. Sci. Eng.* **2012**, *29*, 012019.
- [2] Zerbo, I.; Zoungrana, M.; Ouedraogo, A.; Korgo, B.; Zouma, B.; Bathiebo, D. J. *Global Journal of Pure and Applied Sciences.* **2014**, *20*, 139–148.
- [3] Betsler, Y.; Ritter, D.; Bahir, G.; Cohen, S.; Sperling, J. *App. Phys. Lett.* **1995**, *67*, 1883–1884.
- [4] Vardanyan, R. R.; Kerst, U.; Wawer, P.; Wagemann, H. *Proceeding of 2nd World Conference and Exhibition on Photovoltaic Solar Energy Conversion.* Vienna, Austria, 6–10 July 1998, *Vol I*, p. 191–193.
- [5] Erel, S. *Sol. Energy. Mat. Sol. C.* **2002**, *71*, 273–280.
- [6] Madougou, S.; Made, F.; Boukary, M. S.; Sissoko, G. *Adv. Mater. Res.* **2007**, *18–19*, 303–312.
- [7] Zoungrana, M.; Zerbo, I.; Seré, A. D.; Zouma, B.; Zougmore, F. *Global Journal of Engineering Research.* **2011**, *10*, 113–124.
- [8] Zoungrana, M.; Zerbo, I.; Ouedraogo, F.; Zouma, B.; Zougmore, F. *IOP Conf. Ser.: Mater. Sci. Eng.* **2012**, *29*, 012020.
- [9] Misiakos, K.; Wang, C. H.; Neugroschel, A.; Lindholm, F. A. *J. Appl. Phys.* **1990**, *67*, 321–333.
- [10] Mohammad, S. N. *J. Appl. Phys.* **1987**, *61*, 767–772.
- [11] Barro, F. I.; Sane, M.; Zouma, B. *Turk. J. Phys.* **2015**, *39*, 122–127.
- [12] Diallo, H. L.; Maiga, A. S.; Wereme, A.; Sissoko, G. *Eur. Phys. J. Appl. Phys.* **2008**, *42*, 203–211.
- [13] Mbodji, S.; Ly, I.; Diallo, H. L.; Dione, M.M.; Diasse, O.; Sissoko, G. *Res. J. Appl. Sci. Eng.* **2012**, *4*, 1–7.
- [14] Ly, I.; Ndiaye, M.; Wade, M.; Thiam, N.; Gueye, S.; Sissoko, G. *Res. J. Appl. Sci. Eng. Technol.* **2013**, *5*, 203–208.